Journal of Applied Fluid Mechanics, Vol. 16, No. 12, pp. 2556-2568, 2023.
Available online at www.jafmonline.net, ISSN 1735-3572, EISSN 1735-3645.
https://doi.org/10.47176/jafm.16.12.1814

Effect of Different Types of External Guide Vanes on the Performance of High-Pressure Centrifugal Compressor

P. Niveditha† and B. S. Gopi

Indian Institute of Technology Madras, Madras, Tamil Nadu, 600036, India

†*Corresponding Author Email: me15d406@smail.iitm.ac.in*

ABSTRACT

In order to reduce exit swirl and obtain the desired Mach number, axial exit guide vanes (EGV) are often employed in a centrifugal compressor. NASA CC3 compressor, with wedge vane diffuser and without EGV, is considered as the base model for the analysis and validation. An axial flow domain with exit guide vane is added to this base model after the diffuser outlet to study the effect on the compressor performance. The performance of exit guide vane with different profiles: flat plate, symmetric wedge, circular arc, and airfoil vane profiles by maintaining the same chord, number of vanes, and flow angle of the vanes are studied. Numerical simulations are carried out with 60 number of exit guide vanes for all four types of vanes. Among several combinations, when the centrifugal compressor is equipped with 60 circular arc vanes as EGV, the efficiency and pressure recovery values at the design point have increased by 6.5% and 8.9%, respectively.

Article History

Received February 21, 2023
Revised July 5, 2023
Accepted July 27, 2023
Available online October 8, 2023

Keywords:

Centrifugal compressor
Fluid flow
External Guide Vane (EGV)
Radial diffuser
Turbomachinery

1. INTRODUCTION

Centrifugal compressors are used in more comprehensive applications such as small gas turbines, turbochargers, refrigerators, petrochemical, and process industries. Every application places its demand on the compressor design. A centrifugal compressor with higher efficiency and a more comprehensive operating range is eventually required to be designed. The impeller, diffuser, and volute casing are the significant elements of a centrifugal compressor. The individual component performance needs to be enhanced to maximize the centrifugal compressor stage efficiency. A high-pressure ratio with more significant pressure recovery, more comprehensive operating range, and flow stability are the fundamental aerodynamic performance goals for the compressor. But with the high-efficiency level of the impeller and volute casing already achieved, one has to focus on the diffuser design to improve the overall performance of a centrifugal compressor.

Several diffuser numerical and experimental studies, such as impeller-diffuser interaction, diffuser vane profile, and external guide vane, were performed to aim for the diffuser performance analysis. A three-dimensional non-uniform unstable flow discharged from the impeller is typically transferred to the diffuser. If one wishes to accomplish greater diffuser efficiency over a wide operating range, the effect of the impeller on the diffuser flow in the diffuser design needs to be taken into account. In the present study, to achieve low flow angle and Mach number at compressor exit, external guide vanes are included in the base domain as shown in Fig. 1. External guide vanes (EGV) are included in the compressor domain after diffuser: for further diffusion, guide in a change in the direction of the fluid flow from radial to axial or vice versa, to reduce swirl in the fluid flow and achieve low flow angles. The aim of the axial diffuser in both axial and radial compressors is the same: to further diffuse the flow. However, in some cases of radial EGV, they are also used to change the direction of the flow.

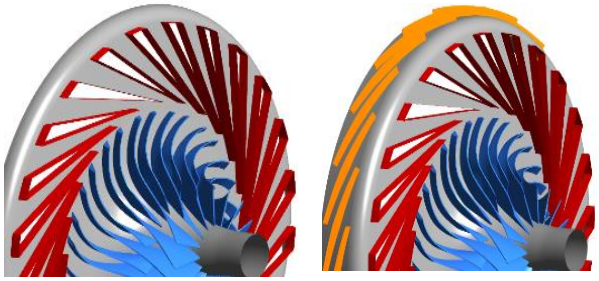

(a) Base Case (b) Base Case with EGV

Fig. 1 NASA CC3 Compressor with and without EGV

Nomenclature

C	Chord	S_E	Energy source
EGV	Exit guide vane	T	Static temperature
EGVA	Axial flow domain with airfoil vane	U	Velocity Magnitude
EGVC	Axial flow domain with circular arc vane	**Subscripts**	
EGVF	Axial flow domain with flat plate vane	1	Compressor inlet
EGVS	Axial flow domain with symmetric wedge vane	2	Impeller outlet /Diffuser inlet
h	Enthalpy	3	Diffuser leading edge
h_{tot}	Total enthalpy	4	Diffuser trailing edge
M	Mach number	5	Compressor outlet
P	Static pressure	**Greek symbols**	
P_0	Total pressure	α	Flow angle
r_0	Total to static pressure ratio	η	Compressor efficiency
S	Entropy	μ	Dynamic viscosity
S_M	Momentum source	τ	Shear stress

In order to evaluate the impact of diffuser stall in the centrifugal compressor, Marsan et al. (2012) conducted the numerical analysis. Their research considered a radial impeller fitted with a radial diffuser, accompanied by an axial diffuser. They concluded that streamlines are mixed on the hub surface, contributing to further losses in the fluid domain. Shumal et al. (2016) used the inverse ball spline algorithm to design the cross-vane diffuser. They also put a cross vane that changes from radial to axial by applying the inverse technique and reducing the total diffuser diameter ratio by 24 percent. They concluded that the updated vane increases efficiency by 2% and decreases secondary losses in the flow domain. Karrabi et al. (2011) used the unique zero 3D method to do their steady and unsteady analysis, which included a radial diffuser followed by external guide vanes. In their analysis, they employed variable coefficients instead of constant coefficients. They concluded that the bend between the radial diffuser and the EGV vane is the primary cause of compressor performance problems.

Benini et al. (2006) used a diffuser with radial and axial vanes to do a numerical study. They refined the profile of EGV vanes by keeping the lower camber and stagger angles. The flow deflection is reduced by maintaining a lower camber angle, which improves compressor performance by minimizing pressure losses. For rotor applications, Medic et al. (2014) designed a higher efficiency centrifugal compressor. For design, they aimed for a low swirl angle and Mach number at the exit of the EGV airfoil vane. The compressor efficiency and pressure recovery are improved by using EGV vanes. By altering the stagger angle, cutting position, and rotation of the angle of the EGV vane, Huang & Tsai (2014) performed numerical analysis. They concluded that the first row of the diffuser vane with a 7.5° stagger angle and the second row with a 5° stagger angle was the best possible combination for achieving high compressor efficiency for their chosen geometry.

In order to study the effect of impeller diffuser interaction on the compressor performance, Shum et al. (2000) performed computational analysis. They had concluded that losses of the impeller tip leakage had shown an effect on the stage pressure rise. They also concluded that losses in the flow domain are high when diffuser vanes are mounted close to the impeller, despite low slip and blockage. Analysis was conducted by Ziegler et al. (2003) by considering various radial gaps between the wedge diffuser and the impeller. They concluded that the small radial gap had shown an improvement in the recovery of diffuser pressure but had shown no impact on the efficiency of the impeller. They also concluded that loading is regulated by small radial gaps on the pressure side of the vane. In contrast, insignificant radial gaps on the pressure side, higher loading with worse diffusion were observed.

By considering compressors coupled with vaneless diffuser and vaned diffuser, respectively, Krain (1981) had conducted experimental research. He noted that the flow is unstable when the diffuser leading edge is placed in the subsonic range. Large wake regions are present in the flow domain between the impeller and diffuser. Gaetani et al. (2012) conducted experiments to examine impeller diffuser flow under off-design conditions such as low and high flow rates. They concluded that total pressure is not affected at high flow rates but has significant drop at lower flow rates.

Experiments with a low-speed centrifugal compressor fitted with a vaned diffuser were conducted by Inoue & Cumpsty (1984). They concluded that when the leading edge of the diffuser vane is positioned nearer to the impeller, the reverse flow in the diffuser domain is observed. The circulation of flow decreases by increasing the number of vanes.

By considering sixteen vaned diffuser configurations, Yoshinaga et al. (1980) conducted experiments. They concluded that the shape of the leading-edge diffuser vane had a significant influence on the fluid flow at the diffuser entrance. By considering the vaned diffuser, Kim et al. (2002) conducted the experimental analysis. They concluded that the diffuser profile had shown a significant influence on the compressor operating range from stall to choke.

Table 1 Geometry details of NASA CC3 compressor

Design flow specifications	
Inlet Total pressure	101352 pa
Total temperature	288.15 C
Design mass flow rate	4.54kg/s
Pressure ratio	4:1
Impeller	
Blade count	Main blades-15
	Splitter blades-15
Impeller speed	21,789rpm
Impeller exit radius (R_2)	215.52mm
Backsweep angle	50°
Shroud tip clearance	0.1524mm (at LE)
	0.61mm (near chord)
	0.203 (at exit)
Diffuser	
Number of vanes	24
Divergence angle	7.8°
R_3	232.97mm
R_4	362.23mm
R_{max}	404.33mm
Diffuser diameter ratio (R_{max}/ R_2)	1.87
External Guide vane	
Blade count	60
The axial length of the vane	65mm

Comparing the traditional vaned diffuser and low solidity vaned diffuser, Holweg et al. (1993), performed experiments. They concluded that the diffuser vane angle for the supersonic compressor, directly impacted the operating range and efficiency of the low solidity vaned diffuser. They also concluded that setting the angle of adverse incidence would help to improve the compressor's stability and performance. By considering the low solidity vaned diffuser, the solidity of 0.69, Eynon & Whitfield (1997) numerically analyzed the effect of vane number and turning angle on compressor performance with low solidity configuration. They had increased number of vanes in the diffuser domain from six to ten. But no effect on the performance of the compressor has been shown. So further, they worked by increasing the turning angle of the vane. They concluded that diffuser efficiency increased due to a decrease in tangential velocity, but volute pressure recovery decreased due to a mismatch of the angle at the trailing edge.

By maintaining solidity in the range of 0.7-0.85, Jangsik et al. (2008) performed a numerical analysis. They took into account the diffuser vane profile as NACA 65 by varying vane stagger angles. They concluded that the 0.803 solidity diffuser with an incidence of -6.28 demonstrated optimal compressor efficiency with a wide operating range. By considering traditional, vaneless, and low solidity vane diffuser setups, Naresh & Engeda (1997) performed experiments. They concluded that the compressor performance could be enhanced using the lower turning angle to the diffuser vane.

As seen from the literature, no studies are reported on the profile study of the EGV vanes. Therefore, the present work objective is to study the impact of different EGV profile in the axial flow domain by considering the NASA CC3 compressor as the base case, as shown in Fig 2.

2. COMPUTATIONAL METHODOLOGY

2.1 Compressor Model

For the present analysis, the NASA CC3 compressor (Medic et al., 2017) is considered as the base configuration. The specifications of geometry and design conditions are shown in Table 1. It is a compressor with a high-pressure ratio and high speed. Nasa CC3 compressor consists of inlet domain, impeller, wedge vane diffuser, and 90° bent Fig. 2.

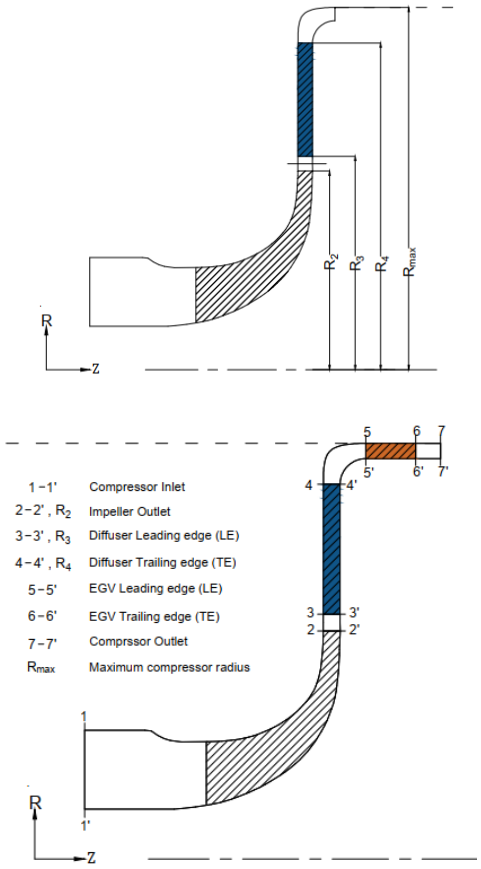

Fig. 2 Meridional view of NASA CC3 compressor with and without EGV

Impeller rotates at the speed of 21,789 rpm. Axial flow domain is added after 90-degree bend of the base case to perform analyses with external guide vanes. Flat plate, airfoil, circular arc, and symmetric wedge, vane profiles are considered to conduct profile studies of external guide vanes shown in Fig 3(a-d). Flow angle (α) is fixed after performing the specific number of simulations at the design flow condition. Further, simulations are conducted in the present analysis by setting the axial length, number of vanes, and flow angle of the EGV vanes. Utilized are flat plate vanes with rounded leading and trailing edges

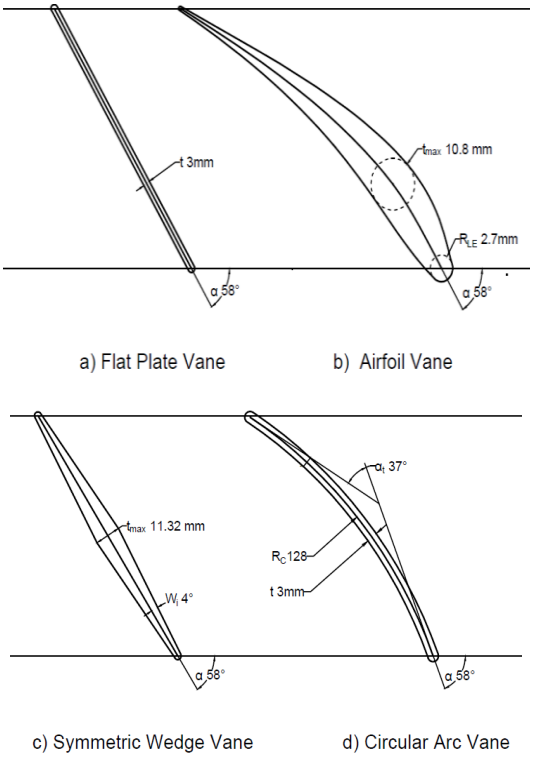

Fig. 3(a-d): Different external guide vane profiles

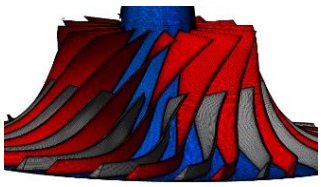

(a) Impeller Mesh

(b) Diffuser Mesh

Fig. 4 CC3 base case impeller and diffuser mesh

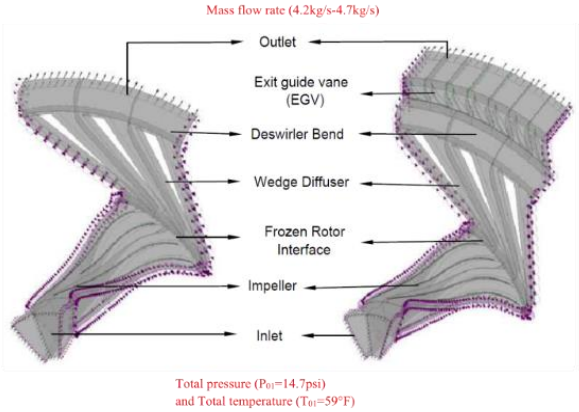

Fig. 5 Single passage of NASA CC3 computational domain

and a uniform thickness of 3mm (refer Fig. 3(a)). The maximum thickness of 10.8 mm and the leading-edge radius of 2.7 mm for NACA 65-4a10 are maintained in the airfoil model. For modelling purposes, symmetric wedge vanes with a maximum thickness of 11.32mm and a wedge included angle of 4° (refer Fig. 3(c)) are used. Wedge included angle is defined as camber to wedge surface, which is shown in (Fig. 3(d)). A circular arc is drawn with one end passing through the Leading Position (LE) and another end being tangent to the Inlet Flow angle. The trailing edge of the profile is fixed in accordance with the necessary turning angle (α_t =37° in present study). By keeping the camber circle's radius at 128mm, a uniform thickness of 3mm was maintained.

2.2 Computational Methodology

For this investigation, ANSYS Bladegen 17.2 is used as the modeling tool. For the development of diffuser blade profiles, the diffuser flow path, flow angle, and thickness distribution along the camber are provided as input parameters. ANSYS Turbogrid 17.2 is used as a mesh tool. The expansion ratio is adjusted such that the value of y+ is less than 2. A single splitter rounded trailing edge topology is employed for impeller vanes, whereas a single round-round symmetric topology is used for diffuser vanes. O-grid mesh is maintained closer to the blade surfaces, while H-grid mesh is generated in the impeller and the diffuser over the fluid flow domain. Figure 4 shows impeller and diffuser mesh corresponding to the base case.

As inlet boundary conditions, total pressure and total temperature (ref. Table.1) are used and at outlet mass flow rate (4.2kg/s-4.7kg/s) is imposed. On the hub wall, shroud wall, and blade profiles of each domain in the centrifugal compressor, a non-slip wall boundary condition was imposed. To save processing time, the fluid domain's side walls are provided with a periodic boundary condition. To maintain adequate pitch between the two fluid domains, the analysis in the current study (Fig. 5) takes into account the two passes of the impeller, three passages of the diffuser, and seven passages of the EGV vanes. Frozen rotor interface is used as the interface between rotor and stator domains.

2.3 Governing Equation

Three-dimensional steady-state simulations are carried out using ANSYS CFX 17.2. After comparison of other turbulence models at design flow conditions (see Table 2) The SST turbulence model is employed in this work (previously used by Ali et al. 2017), using air as the fluid medium. Because it can predict the degree of flow separation under unfavorable pressure gradients, the Shear Stress Transport (SST) k-omega turbulence model was chosen. The transfer of turbulent shear stress in this model accounts for turbulence viscosity. Numerical and advection schemes are set to a double mode of precision and high resolution. High resolution is a second order upwind bias discretization approach for solving governing equations with shocks and discontinuities. Total energy is used as heat transfer method. The mass,

Momentum, and energy governing equations imposed on the ANSYS CFX 17.2 solver are listed in Eq. 1-5.

Table 2 Comparison of different turbulence models at design flow

Model	Isentropic efficiency (η)	Total to static pressure ratio (r_0)
SST	83.19	3.98
K-epsilon	82.00	3.75
K-omega	82.99	3.95
Eddy viscosity transport equation	84.50	4.15

When the total of the residuals for mass, momentum, and energy is less than 10-5, simulations are considered to converge. Additionally, we have always ensured that efficiency and mass flow monitor plots had reached a constant value before the simulation run was terminated in ANSYS CFX residuals.

Continuity Equation:

$$\frac{\delta \rho}{\delta t} + \nabla.(\rho, U) = 0 \tag{1}$$

Momentum Equation:

$$\frac{\delta(\rho U)}{\delta t} + \nabla.(\rho U.U) = -\nabla p + \nabla \boldsymbol{\tau} + S_M \tag{2}$$

$$\tau = \mu(\nabla U + (\nabla U)^T - \frac{2}{3}\delta \nabla.U \tag{3}$$

Total Energy Equation:

$$\frac{\partial(\rho h_{tot})}{\partial t} - \frac{\partial \rho}{\partial t} + \nabla.(\rho U h_{tot}) = \nabla.(\lambda \nabla T) + \nabla.(U.\boldsymbol{\tau}) + U.S_M + S_E \tag{4}$$

$$h_{tot} = h + \frac{1}{2}U^2 \tag{5}$$

For the present analysis, Table 2 displays the numerical matrix. The total pressure and total temperature at the inlet and at outlet mass flow rates are given as boundary conditions. The mass flow rate was varied from 4.7kg/s to 4.2kg/s in 0.1kg/s increments to evaluate the impact of EGV on the compressor domain from maximum to minimum flow rate conditions.

2.4 Grid Independent Study

Simulations are carried out by considering the coarse (1.7 million), medium (2.2 million), and fine (2.8 million) mesh sizes for the base case (Experimental data) in order to ensure the results are independent of mesh dimension. For various mesh sizes, Fig. 6 gives information on the pressure ratio and efficiency for the entire operating range of the compressor. It can be seen from Fig. 6 that the outcomes of the medium and fine mesh are almost identical. Therefore, for the current research, medium mesh size components are used.

2.5 Numerical Validation

By taking into account the experimental findings by Lurie et al. (2011), numerical validation for the NASA

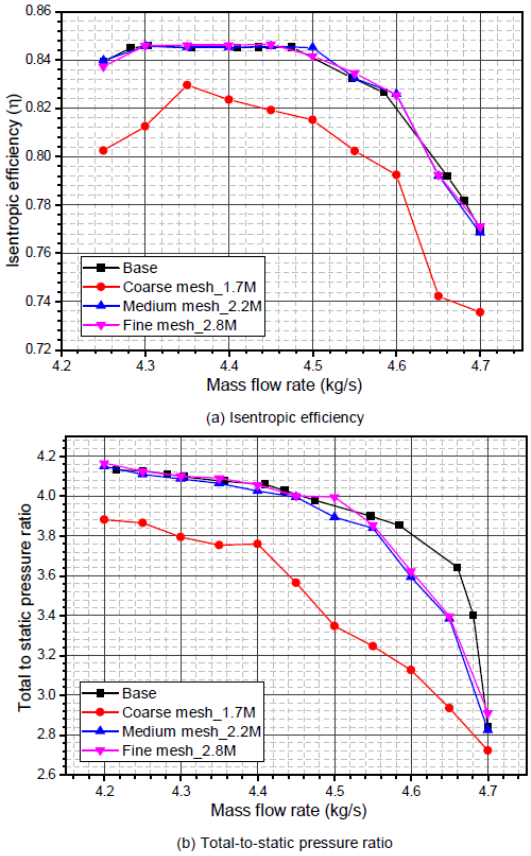

Fig. 6 Grid independence study from minimum-maximum flow condition

CC3 compressor is carried out in the current work. To compare the performance differences between experimental and numerical results from minimum - maximum flow zones, the total to static pressure ratio and isentropic efficiency are taken into consideration. Plots comparing experimental and CFD results are shown in Fig. 7.

At lower flow rates and maximum flow, the total-static pressure ratio showed good agreement, although a minor variation is seen around design flow. However, the results of CFD and experiments from minimum-maximum flow locations showed a good agreement in the case of isentropic efficiency. The authors are now able to perform more numerical analysis since we are more assured about the numerical results we had obtained.

3. RESULT AND DISCUSSION

Steady-state simulations are carried out by considering the NASA CC3 compressor as the base case. The following section plots performance characteristics to find the effect of change in compressor performance by adding external guide vanes to the diffuser. The order of the results discussion is as follows: 1) base case 2) base case with EGV flow domain 3) performance characteristics plots and followed by conclusions drawn from the present work. For the significant parameters in the present work and computational matrix refer to Table 3.

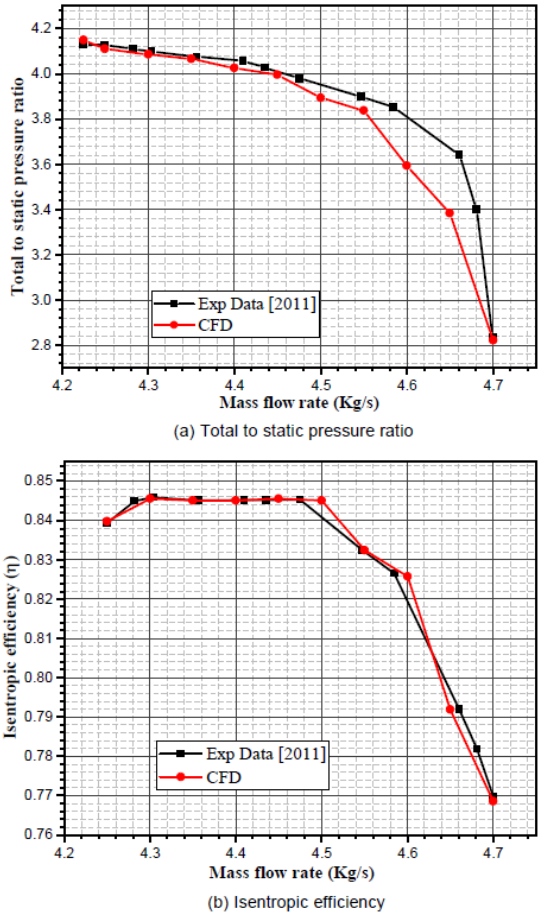

Fig. 7 Numerical validation of the present study

Table 3 Computational matrix

Case	Parameter			No. of cases
	Profile	Vane number	Offset and flow angle	
Base case	-			11
Base case with EGV.	Airfoil (EGVA)	60	2 offset	1
		60	4 offset	1
		60	α =54	1
		60	α =58	1
		60	4 offset, α =58	7
	Flat plate (EGVF)	60	4 offset, α =58	7
	Symmetric wedge (EGVS)	60	4 offset, α =58	7
	Circular arc (EGVC)	60	4 offset, α =58	7

3.1 Base Case

The static and total pressure, Mach number, and velocity flow angle plots for the base case at the design mass flow condition are shown in Fig. 8. Plots are aggregated from diffuser inlet to outlet along the streamwise location (2-3 VL, 3-4 wedge diffuser, 4-5 90-degree bend).

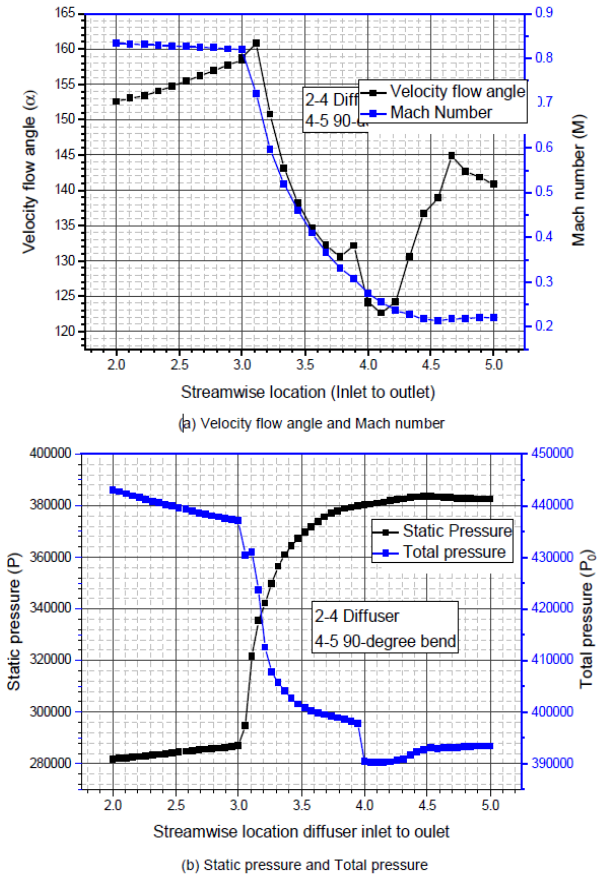

Fig. 8 Static and total pressure, velocity flow angle, mach number along the stream wise direction

3.2 External Guide Vane (EGV)

An axial flow domain is included to the base case compressor, after a 90-degree bend; refer to Fig 1(b). To fix the flow angle of the EGV blade, simulations are performed with 2° offset vane, 4° offset vane, flow angles (α) =54°, =58°, and 4° offset with a 58° flow angle vane. To investigate the influence of the external guide vanes flow angle on compressor performance, airfoil vanes are put in the axial flow domain. Figure 9 depicts the angles taken into account while creating an EGV vane profile. Offset is defined as varying the relative position of EVG vane with respect to diffuser vane in theta direction. Figure 10 shows the pressure ratio and isentropic efficiency for the five different cases with EGV airfoil vane at design mass flow condition (=4.54 kg/s). It is seen from the performance plots that pressure rise increases by adding axial flow domain with vanes for all the cases. Out of all the possibilities, 4° offset, and flow angle (α) = 58° had

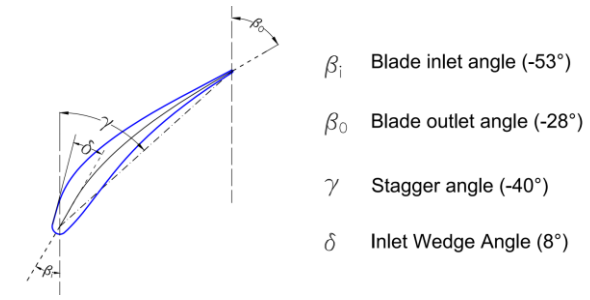

(a) Airfoil Blade Profile with Vane Angles

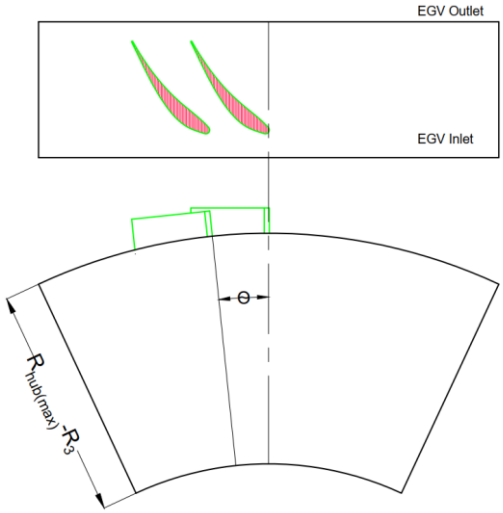

(b) Definition of Offset

Fig. 9 (a-b) Angle consideration for EGV profile vane

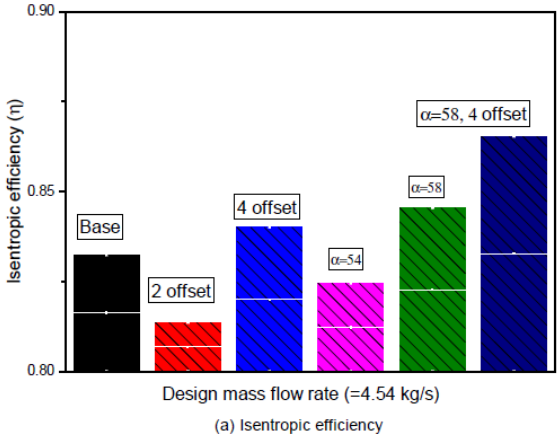

(a) Isentropic efficiency

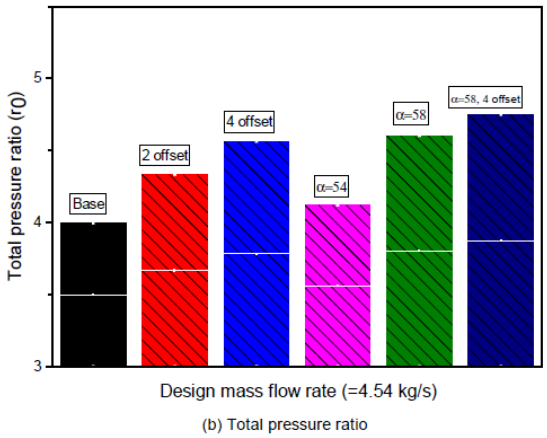

(b) Total pressure ratio

Fig. 10 Total pressure ratio and isentropic efficiency at design flow condition with different flow angles

shown optimum performance in a pressure rise and efficiency increase.

Therefore, in the present study for further investigations of profile study, simulations are carried out by placing the vane at 4° offset with a 58° flow angle.

Further simulations are carried out by considering flat plate vane, symmetric wedge vane, and circular arc vanes to study the effect of different vane profiles in EGV performance. To evaluate the performance improvement of the modified compressor with EGV and the base case, the following characteristics: Total pressure ratio (r0), Isentropic efficiency (η), static pressure recovery coefficient (CP), pressure contours, velocity streamlines, eddy viscosity, Mach number, and velocity flow angle(α) are discussed in the following.

3.2.1 Total Pressure Ratio

Figure 11 and Table 4 exhibit pressure charts for various mass flow conditions, along with a proportional rise or reduction in pressure in relation to a base case. The total pressure ratio is defined as the total pressure at the EGV outlet to the total pressure at compressor inlet. It is observed from the plots that the rate of increase in total pressure is higher for EGV with airfoil vane (EGVA) and EGV with circular arc vane (EGVC) at design flow conditions compared to a base case by 20.9% and 21.7%, respectively. In case of symmetric wedge vanes, total pressure ratio is higher at design flow condition but poorer at extreme conditions compared to the base case. But in EGV with flat plate vanes (EGVF), the pressure rise is lower compared to the base case for the entire flow range (Refer Table 4). At extreme flow conditions, the increase in pressure ratio is lower than in other operating conditions.

Circular arc profile vanes (EGVC) and airfoil vanes (EGVA), as seen in Fig. 11, performed better than base case at minimum flow rate (=4.2kg/s). Utilizing symmetric wedge vanes (EGVS) and flat plate vane (EGVF), poor performance was attained. Similar trends in performance were seen at maximum flow rates (=4.7kg/s),

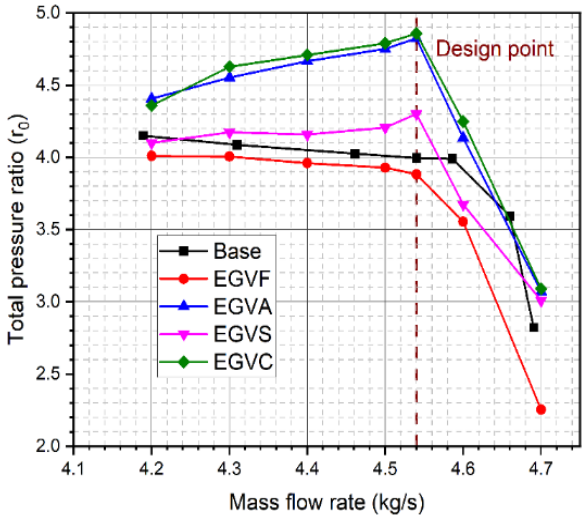

Fig. 11 Total pressure ratio vs mass flow rate

Table 4 Percentage increase or decrease of r_0

m(kg/s)	EGVF	EGVA	EGVS	EGVC
4.7	-20.1	8.8	6.6	9.5
4.6	-1.1	15.0	2.2	18.2
4.54	-2.7	20.9	7.8	21.7
4.5	-1.7	18.9	5.3	19.9
4.4	-1.6	15.9	3.3	17.0
4.3	-2.0	11.4	2.1	13.2
4.2	-3.4	5.2	-1.2	5.0

where EGVC and EGVA enhanced performance while EGVF and EGVS diminished it relative to the base case in terms of total pressure ratio.

3.2.2 Pressure Recovery Coefficient (C_P)

The static pressure recovery coefficient for the diffuser is defined as the change in static pressure rise across the diffuser to the dynamic pressure. Static pressure recovery across the diffuser with EGV airfoil vane (EGVA) and EGV with circular arc vane (EGVC) is higher for the entire flow range than the base model. For EGVA and EGVC, the static pressure recovery increases by 4.2%-8.0% and 6.6%-10.3%, respectively, for different flow conditions, refer (to Table 5 and Fig. 12). In the situations of EGVC and EGVA, the diffuser passage area is growing from intake to outlet, which resulted in a decrease in velocity and a larger pressure recovery. In contrast, the flow area of symmetric wedge vanes decreases until the middle section of the vane and then increases from the middle section to the outlet, where the flow first accelerates then decelerates. The flow area is increasing from the EGVF inlet to the outlet, but the flow is not properly guided in the diffuser domain. In cases of EGV with flat plate vane (EGVF) and EGV with symmetric wedge vane (EGVS) the static pressure recovery decreases for the entire flow range compared to the base model. For EGVF and EGVS the static pressure reduces by 2.6%-9.2% and 0.5%-1.0%, respectively.

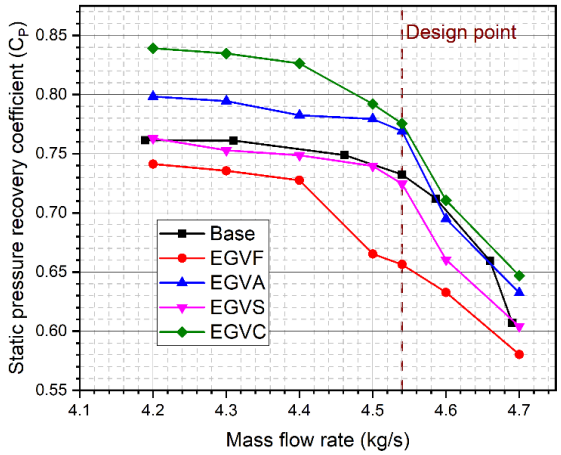

Fig. 12 Static pressure recovery coefficient vs mass flow rate

Table 5 Percentage increase or decrease of C_p

m(kg/s)	EGVF	EGVA	EGVS	EGVC
4.7	-4.4	4.2	-0.5	6.6
4.6	-4.0	5.4	0.1	7.8
4.54	-7.8	8.0	1.7	8.9
4.5	-9.2	6.4	1.0	8.1
4.4	-2.8	4.5	0.0	10.3
4.3	-3.4	4.4	-1.1	9.7
4.2	-2.6	4.8	0.2	10.2

3.2.3 Isentropic Efficiency (η)

Isentropic efficiency (η) of the compressor is defined as the ratio of isentropic work to actual work done by the compressor. Figure 13 and Table 6 show that the isentropic efficiency for the EGV with flat plate vane (EGVF) and EGV with symmetric vane (EGVS) is lower for the entire flow range than the base model. For EGVF and EGVS the isentropic efficiency decreases by 4.4%-dyn6.3%, 0.2%-3.1%, respectively.

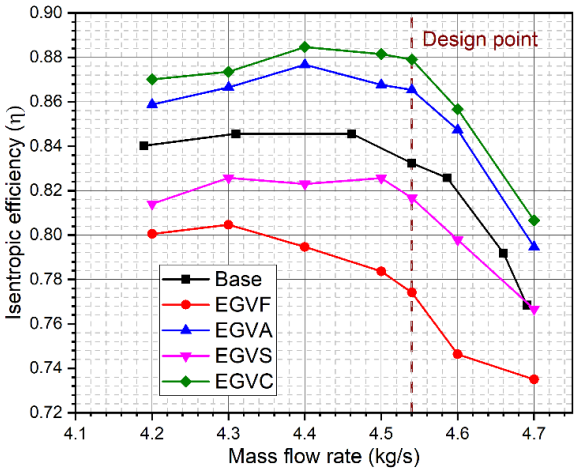

Fig. 13 Isentropic efficiency vs mass flow rate

Table 6 Percentage increase or decrease of η

m(kg/s)	EGVF	EGVA	EGVS	EGVC
4.7	-4.4	3.4	-0.2	5.0
4.6	-5.8	7.0	0.8	8.2
4.54	-6.3	4.8	-1.1	6.5
4.5	-5.9	4.2	-0.8	5.9
4.4	-6.0	3.7	-2.7	4.6
4.3	-4.8	2.5	-2.3	3.3
4.2	-4.7	2.2	-3.1	3.6

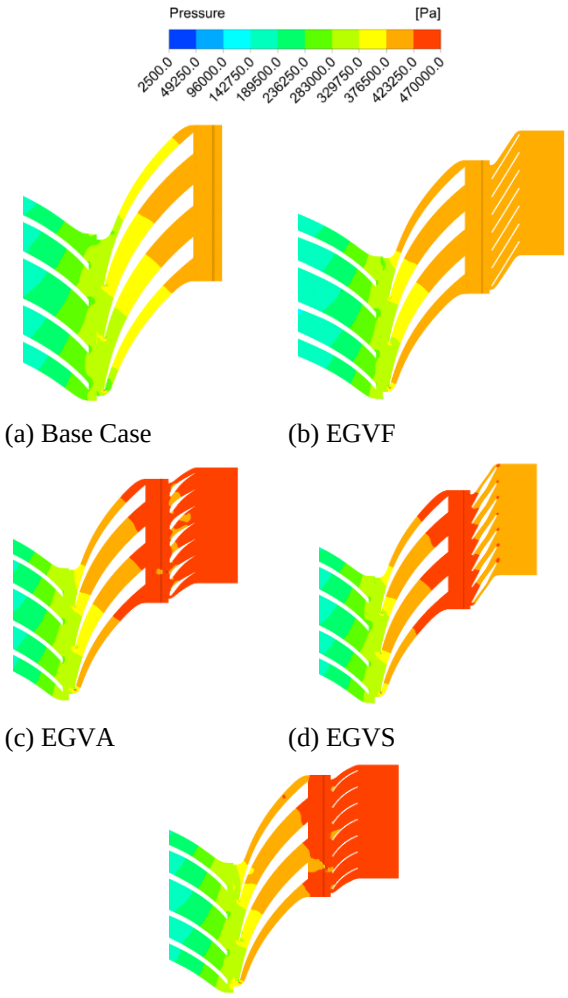

(a) Base Case (b) EGVF

(c) EGVA (d) EGVS

(d) EGVC

Fig. 14 Static pressure contour at 50% constant span

But in the cases of EGV with airfoil vane (EGVA) and EGV with circular arc vane (EGVC) the efficiency increases for the entire flow range compared to the base model. In EGVA and EGVC, the isentropic efficiency (η) increases by 2.2%-7.0%, 3.3%-8.2%, respectively. While EGVF and EGVS performance was decreased by 4.4 percent and 0.2 percent, respectively, at maximum flow rate (=4.7kg/s), EGVC and EGVA efficiency were increased by 5 percent and 3.4 percent, respectively. Similar trends are seen under minimum flow conditions, where EGVC and EGVA perform better and EGVF and EGVS perform poorer.

3.2.4 Static Pressure Contour (P)

Static pressure contours are plotted in the compressor domain at a 50% constant span in the blade-to-blade view shown in Fig. 14. The increase in static pressure is higher in EGV with airfoil vane (EGVA), and EGV with circular arc vane (EGVC) is higher than the base case. No increase in static pressure is noted in cases of EGV with flat plate vane (EGVF) and EGV with symmetric vane (EGVS) cases. From the contours, it can be deduced that the kind of EGV vane profile has an impact on the rate of increase in static pressure rise.

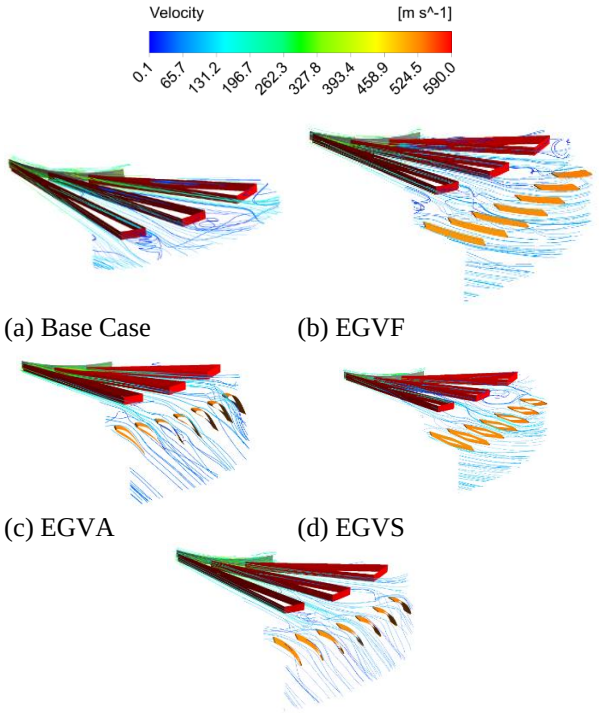

(a) Base Case (b) EGVF

(c) EGVA (d) EGVS

(d) EGVc

Fig. 15 Velocity streamlines in the diffuser fluid domain

As the type of the vane influences the fluid area in the diffuser domain, the profile vane shape has been proven to have an impact on the static pressure rise in the diffuser domain. In the cases of EGVF, EGVC, and EGVA, the flow area increased from the diffuser's inlet to its outlet. Regardless of the fact that the flow area is increasing in the case of the EGVF, the pressure recovery is lower because the flow coming from the deswirler bend is not as well controlled. The same pattern of increase in static pressure is also noticed in static pressure recovery coefficient (Cp) refer Fig 12.

3.2.5 Velocity Streamlines

Velocity streamlines are plotted in the fluid diffuser domain from inlet to outlet as shown in Fig. 15. The length of streamlines should be lower to overcome the frictional losses in the fluid field and to obtain better performance. It can be noted from Fig .15(a) that the mixing is very high in the 90 ° bend. In cases of EGV with airfoil vane (EGVA) and EGV with circular arc vane (EGVC), the mixing of the streamlines is lower in a 90-degree bend which infers that the flow is controlled well by placing EGVA and EGVC in diffuser domain. Since the non-uniform streamlines is reduced in EGVC and EGVA cases and so they had obtained better performance in terms of efficiency and pressure recovery. As the non-uniform streamlines is higher in cases of EGV flat plate vane (EGVF) and EGV symmetric wedge vane (EGVS), the isentropic efficiency (η) is lower in these cases compared to other cases refer Fig. 13. The streamlines in the EGVF and EGVS are longer than in the other two cases, resulting in increased energy loss in these conditions. In the EGV fluid domain, the geometry of the EGV vane profile has a significant impact on the streamlines.

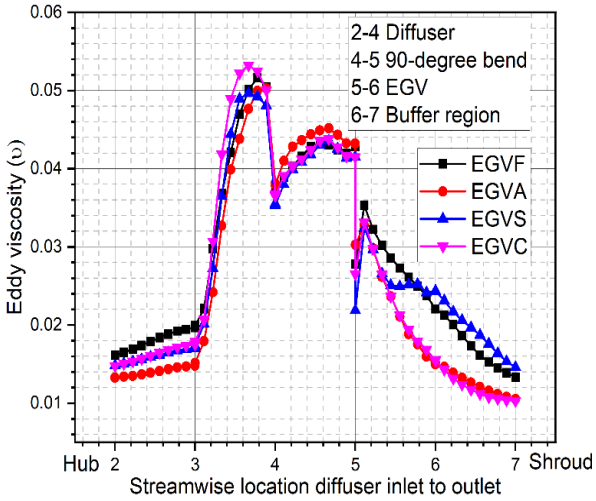

Fig. 16 Eddy viscosity chart from diffuser inlet to compressor outlet

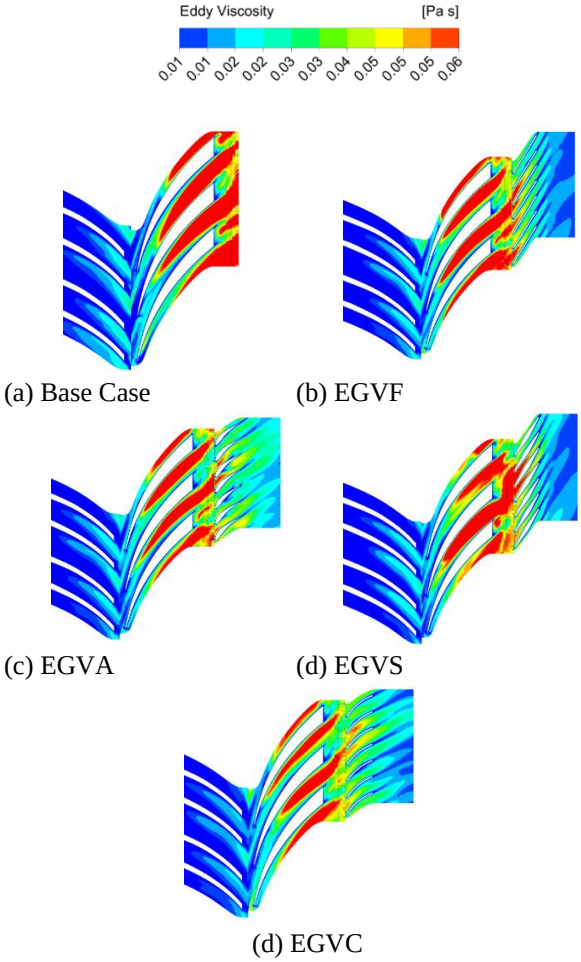

Fig. 17 Eddy viscosity contour at 50% constant span in the blade-to-blade view

3.2.6 Eddy Viscosity

Eddy viscosity contours and charts are plotted in the diffuser fluid domain from inlet to outlet at 50% constant span blade to blade view. The eddy generation rate is higher in the diffuser domain, which can be noted from Fig 16 and Fig 17. The fluid domain has no negative eddy viscosity, as seen by the contours. When negative viscosity generation occurs in the fluid domain, Jiang et al. (2020) suggest that eddy transport equations plays major role in evaluating performance.

By adding an axial flow domain with vanes, eddy viscosity decreases for all the EGV vanes. Among all the cases, EGV with circular arc vane (EGVC) and EGV with airfoil vane (EGVA) have low eddy viscosity compared to other cases. The eddy viscosity generation is lower as the flow is guided well by EGVA and EGVC the losses are lower in the diffuser domain.

The primary reason for the decrease in eddy viscosity in the EGV flow domain is the decrease in flow angle, which results in lower tangential velocity and hence improved compressor performance. Out of all the cases, EGVA and EGVC have low losses in the diffuser fluid domain. Placing EGV vanes in the axial domain also minimizes viscosity generation in the 90-degree curve. In diffuser wedge vanes, the influence of putting EGV vanes on eddy viscosity generation is lower.

3.2.7 Velocity Flow Angle

Velocity flow angle (α) charts are plotted from diffuser inlet to outlet in the stream wise location. Flow angle charts are plotted by using ANSYS CFD post turbo mode from inlet to outlet in the fluid domain. X-axis is considered as stream wise location whereas Y-axis is considered as circumferentially area averaged flow angle refer Fig 18(a). Flow angle in the fluid domain should be optimum to maintain a lower tangential velocity component and a higher radial velocity component. By adding EGV with airfoil vane (EGVA) and EGV with circular arc vane (EGVC) the flow angle decreases along with the flow domain from EGV inlet to outlet. No change in the flow angle for EGVF and EGVS was noticed in Figs 18(a).

Out of all the cases, the flow angle is lower for EGVC and followed by EGVA. Figure 18(b) shows velocity flow angle charts plotted at the diffuser vane's leading and trailing edges from the hub to the shroud. In Fig 18(b) the flow angle curve at leading edge was superimposed in cases of EGVF and EGVS. The major goal of adding an EGV vane is to reduce swirl in the diffuser domain following a 90-degree bend, which was accomplished by lowering the flow angle of the EGVC and EGVA vanes. EGVF and EGVS vanes did not achieve the goal of placing EGV vanes since there was no decrease in the velocity flow angle. Low flow angles are aimed at diffuser outlet for better performance, and in the present analysis low flow angle was achieved by placing circular arc profile vanes in the diffuser domain.

3.2.8 Mach Number

Mach number contours are plotted at a 50% constant span in the blade-to-blade view at the design flow condition shown in Figs 19 and 20. The primary objective of adding axial flow domain and placing vanes is to control the flow angle and achieve a low Mach number at the compressor outlet. As the type of vane profile governs the fluid flow area, in the case of symmetric wedge vane, the flow area decreases then increases, leading to an

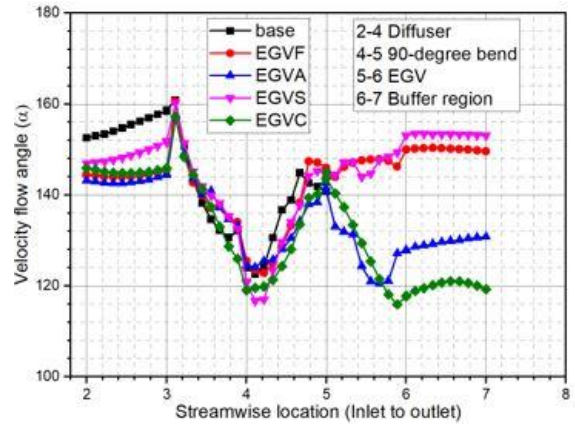

(a) Velocity flow angle from diffuser inlet to outlet

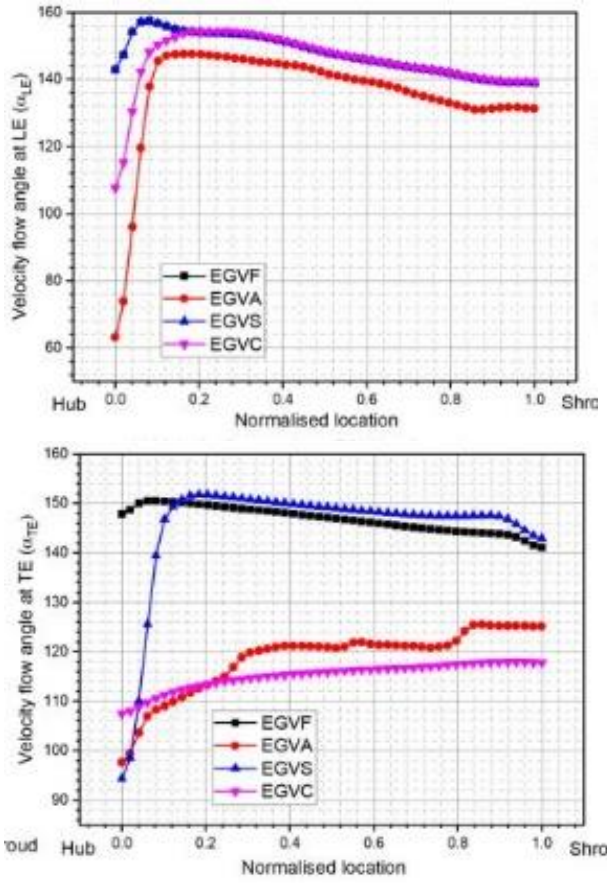

(b) Velocity flow angle at EGV leading and trailing edge

Fig. 18(a-b) Velocity flow angle

increase and decrease of the Mach number in the case of EGV symmetric wedge profile (EGVS). The reduction of the Mach number is more in the EGV with circular arc profile (EGVC) and EGV with airfoil profile (EGVA) compared to the base case. When EGVF and EGVS are compared to the basic case, there is no noticeable difference in Mach number. In the diffuser wedge vanes, no significant change in Mach number was found after introducing EGV vanes (Fig. 19). The Mach number contours and chart show that the Mach number is same for the compressor diffuser vanes with and without EGV vanes, with the exception that the influence of EGV vanes starts at the compressor 90-degree bend.

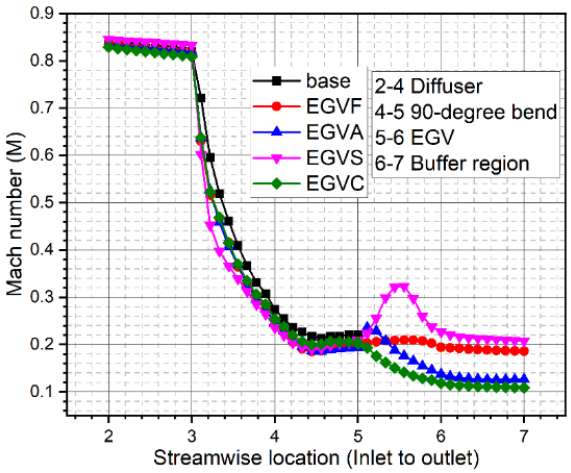

Fig. 19 Mach number plots from diffuser inlet to outlet

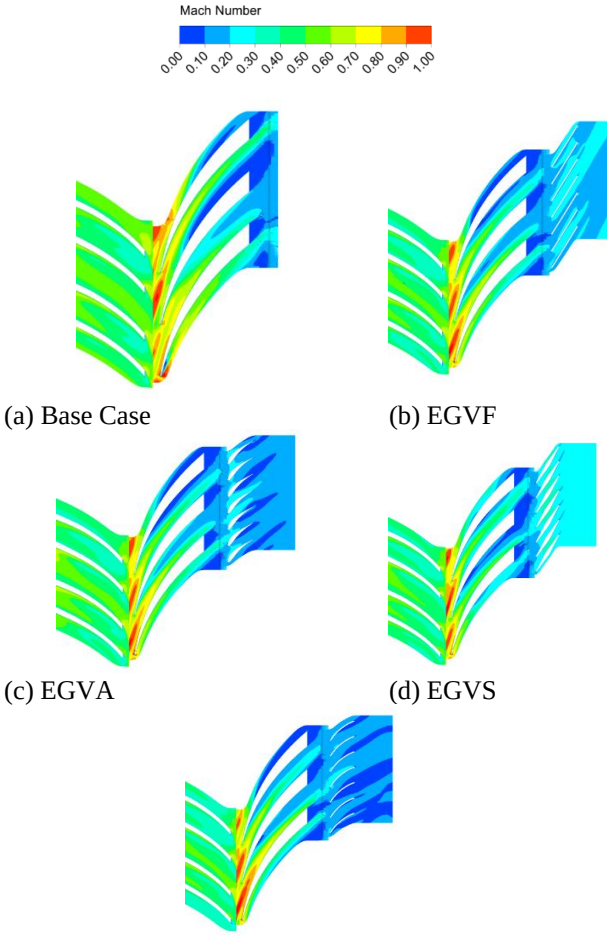

(a) Base Case (b) EGVF

(c) EGVA (d) EGVS

(d) EGVC

Fig. 20 Mach number contour at 50% constant span at design flow condition

4. CONCLUSIONS

By considering the NASA CC3 compressor as the base case, three-dimensional steady-state simulations are performed. The base case considered for the current analysis consists of the impeller, wedge vane diffuser, and 90-degree bend. For the base case, the standard diffuser diameter ratio is 1.87. Compressor efficiency and pressure

ratio were found to be 83.1% and 3.9, respectively, for the base case at the design point.

The present work aims to investigate the performance of the base case by providing the diffuser with an external guide vane under conditions: base case coupled with different EGV vane profiles such as Airfoil vane, circular arc vane, flat plate vane, and symmetric wedge vane. The best cases for optimum efficiency and pressure recovery are identified. The key conclusions taken from this analysis are the following:

1. Circular arc and airfoil vane profiles have shown an increase in static pressure recovery by 6.6%-10.3% and 4.2% and 8.0%, respectively. By adding symmetric wedge vanes in the EGV domain, the pressure ratio of the compressor decreases as the flow area between the vanes is reduced.

2. Isentropic efficiency of the compressor is improved by adding circular arc and airfoil vanes by 3.3%-8.2% and 2.2%-7.0%, respectively. In contrast, in the flat plate (EGVF) and circular arc (EGVC) vane profiles, efficiency decreased compared to the base case.

3. Adding EGVF and EGVS vanes to the axial domain does not enhance compressor performance since these vanes have shown no impact on lowering flow angle in the diffuser fluid domain and also increases eddy viscosity formation. The compressor performance decreases as a result of all of these issues together.

4. The Mach number at the compressor exit is reduced by 50% by providing the axial flow domain to the base case. The non-uniform streamlines is controlled in the EGV fluid domain by adding circular arc and airfoil vanes because the flow is guided well not only in the EGV fluid domain but also in the 90-degree bend.

CONFLICT OF INTEREST

Authors have no conflicts to disclose.

AUTHORS CONTRIBUTION

Porika Niveditha is the primary author and is responsible for conceptualization, formal analysis, investigation, and drafting the original draft. Gopi BS, a co-author, assisted in the formulation of methodology and the revision of the draft.

ACKNOWLEDGEMENTS

Authors would like to acknowledge Late. Prof. B. V. S. S. S. Prasad for his contribution and insightful comments on the work.

REFERENCES

Ali, Z., Lee, B. J. & Chung J. T. (2017). Numerical evaluation of transient flow characteristics in a transonic centrifugal compressor with vaned diffuser. *Aerospace Science and Technology*, 70, 244-256. https://doi.org/10.1016/j.ast.2017.08.003

Benini, E., Toffolo, A. & Lazzaretto A. (2006). Experimental and numerical analyses to enhance the performance of a microturbine diffuser. *Experimental Thermal and Fluid Science*, 30 (5), 427-440. https://doi.org/10.1016/j.expthermflusci.2005.09.003

Eynon, P. A., & Whitfield, A. (1997). The effect of low-solidity vaned diffusers on the performance of a Turbocharger compressor. Proceedings of the Institution of Mechanical Engineers, Part C: Journal of Mechanical Engineering Science, 211(5), 325–339. https://doi.org/10.1243/0954406971522088

Gaetani, P., Persico, G., Mora, A., Dossena, V., & Osnaghi, C. (2012). Impeller-Vaned diffuser interaction in a centrifugak compressor at off design conditions. *ASME Journal of Turbomachinery*, 134/061034, 1-9. https://doi.org/10.1115/GT2011-46234

Holweg, W. C., Direnzi, G. L., & Aungier, R. H. (1993). Comparison of conventional and low solidity vaned diffusers. *ASME*, 93-GT-98. https://doi.org/10.1115/93-GT-098

Huang, J. M., & Tsai, Y. H. (2014, January). Design and analysis of a split deswirl vane in a two-stage refrigeration centrifugal compressor. *Advances in Mechanical Engineering.* https://doi.org/10.1155/2014/130925

Inoue, M., & Cumpsty, N. A. (1984). Experimental study of centrifugal impeller discharge flow in vaneless and vaned diffusers. *Journal of Engineering for Gas Turbines and Power*, 106/455-467. https://doi.org/10.1115/1.3239588

Jiang, N., William, L., Michael, Mc., Yao, R., & Haiyun, Z. (2020). On the foundations of eddy viscosity models of turbulence. *Fluids*, 2311-552, https://doi.org/10.3390/fluids5040167.

Jongsik, O., Buckley, C. W., & Agarwal Gril, L. (2008). *Numerical investigation of low solidity vaned diffuser performance in a high-pressure centrifugal compressor, Part II: Influence of vane stagger*. Proc. of ASME Turbo Expo, Berlin, Germany, GT2008-501178. https://doi.org/10.1115/gt2008-50178

Karrabi, H., Pourfarzaneh, H., & Hajilouy-Benisi. (2011, November 11–17). *Zero D and 3D analysis of the centrifugal compressor of a gas turbine and its evaluation using experimental results.* Proc of ASME International Mechanical Engineering Congress and Exposition, Colorado, USA.

Kim, Y., Engeda, A., Aungier, R., & Amineni, N. (2002). A centrifugal compressor stage with wide flow range vaned diffusers and different inlet configurations. *Proceedings of the Institution of Mechanical Engineers, Part A: Journal of Power and Energy*, 216, 307-320. https://doi.org/10.1243/09576500260251156

Krain, H. (1981). A study on centrifugal impeller and diffuser flow. *ASME Journal of Engineering for Power*, 103, 688-697. https://doi.org/10.1115/1.3230791

Lurie, E. A., Slooten, P. R. V., Medic, G., Mulugeta, J. M., Holley, B. M., Feng, J., and Sharma, O. (2011). *Design of a high efficiency compact centrifugal compressor for rotorcraft applications*. American Helicopter Society 67th Annual Forum, Virginia Beach, USA.

Marsan, A., Isabelle, T., Sylvain, C., & Leroy, G. (2012). Study and control of a radial vaned diffuser stall. *International Journal of Rotating Machinery*, https://doi.org/10.1155/2012/549048

McKain, T. F., & Holbrook, G. J. (1997, July). Coordinates for a High Performance 4:1 Pressure Ratio Compressor," NASA CR-204134.

Medic, G., Sharma, O., Jongwook, J., Hardin, L. W., McCormick, D. C., Cousins, W. T., Lurie, E. A., Shabbir, A., Holley, B. M., & Van Slooten, P. R. (2014, November). *High efficiency centrifugal compressor for rotorcraft applications*. NASA/CR—2014-218114.

Naresh, K., & Engeda, A. A. (1997*). Pressure recovery in low solidity vaned diffuser for centrifugal compressors*. https://doi.org/10.1115/97-GT-472.

Shum, Y. K. P., Tan, C. S., & Cumpsty, N. A. (2000). Impeller-diffuser interaction in a centrifugal compressor. *ASME Journal of Turbomachinery*, 122(4), 777–786. https://doi.org/10.1115/1.1308570

Shumal, M. A., M. Nili-Ahamadabadi, & E. Shirani. (2016). *Quasi-3d inverse design of a vaned 90-degree bent diffuser for the Exit of a centrifugal compressor impeller*. Proc of ASME Turbo Expo, Seoul, South Korea, GT2016-57881

Yoshinaga, Y., Gyobu, I., Mishina, H., Koseki, F., & Nishida, H. (1980). Aerodynamic performance of a centrifugal compressor with vaned diffusers. *ASME Journal of Fluids Engineering*, 102, 486-493. https://doi.org/10.1115/1.3240730

Ziegler Kai, U., Gallus Heinz, E., & Niehuis, R. (2003). A study on impeller-diffuser interaction - part ii: detailed flow analysis. *ASME Journal of Turbomachinery*, 125, 183-192. https://doi.org/10.1115/1.1516815